

Silicon Detector Studies with an Interferometric Thickness Mapper

Barrett Milliken¹, Richard A. Leske², and Mark E. Wiedenbeck¹

¹*Jet Propulsion Laboratory,* ²*California Institute of Technology*
Pasadena, California U S A

Abstract

A laser-interferometer system has been developed to precisely map the thickness variations of large-area silicon detectors. We describe the design and operation of the apparatus and the data processing carried out to derive thickness maps. We compare the results with a map made using accelerator beams of energetic heavy ions.

1. Introduction

Cosmic ray isotopic composition studies aboard satellites are normally based on measurements of ΔE vs. total energy in a stack of silicon solid-state detectors. This technique requires a precise knowledge of the matter thickness, L , penetrated by each particle. An uncertainty in L contributes an uncertainty in the derived particle mass, M , according to $\sigma_M/M \simeq 1.4 \sigma_L/L$. Thus for an ^{56}Fe nucleus penetrating a 500 pm thick ΔE detector, the thickness must be known to 0.6 μm or better in order for the thickness uncertainty to not contribute more than 0.1 amu to the mass resolution. Since the thickness variations of commercially available silicon detectors are commonly greater than the maximum allowable thickness error, it is necessary to map the detector thickness as a function of position on the detector.

The Solar Isotope Spectrometer (SIS) which is being developed for the NASA Advanced Composition Explorer (ACE) mission [1] requires mapping of 60 large-area (65 cm^2) ion-implanted silicon detectors with nominal thicknesses ranging from 100 μm to 1000 μm . Thickness mapping using accelerator beams of heavy ions requires large amounts of beam time and entails a very extensive data analysis effort. In order to simplify the detector mapping task for SIS we have developed a dual laser interferometer system capable of making automated, high-precision measurements of detector thickness variations. Studies have been made of the performance of this installment, including comparisons with accelerator maps of the same detectors.

2. Interferometer Design

Figure 1 shows a schematic illustration of the components of the interferometer system. The two portions enclosed in dashed boxes are Michelson interferometers (labeled IF1 and IF2), each used to compare the distance between an "interference splitter" and one surface of the detector with the fixed distance between that splitter and a reference mirror. The interference between the recombined beams is processed with a commercial receiver and signal analysis electronics (Hewlett-Packard models 10780C and 5527, respectively) which continuously track changes in the relative lengths of the two

arms[2]. The rest of the optics are used to obtain the input laser beams for the two interferometers from a single He-Ne laser.

The detector being tested is mounted on a two-dimensional computer-controlled stage capable of moving the detector in the plane perpendicular to the laser beams. As the detector is moved, the sum of the signals from the two interferometers provides a measurement of $(L'_1 + L'_2) - (L_1 + L_2)$ (see Fig. 1). The sum of the distances to the two surfaces of the detector ($L'_1 + L'_2$) varies from point to point on the detector due to the thickness variations, while the reference sum ($L_1 + L_2$) remains constant. Note that because distances to the two detector faces are obtained simultaneously, the thickness measurement is very insensitive to movements of the detector along the direction of the laser beam.

The mechanical structure which defines the two arms of the interferometers is constructed of invar to minimize dimensional changes with temperature, and lengths of all the arms are designed to be equal ($L_1 = L'_1 = L_2 = L'_2$) in order to compensate for residual thermal expansion and time variation of the air density in the optical path.

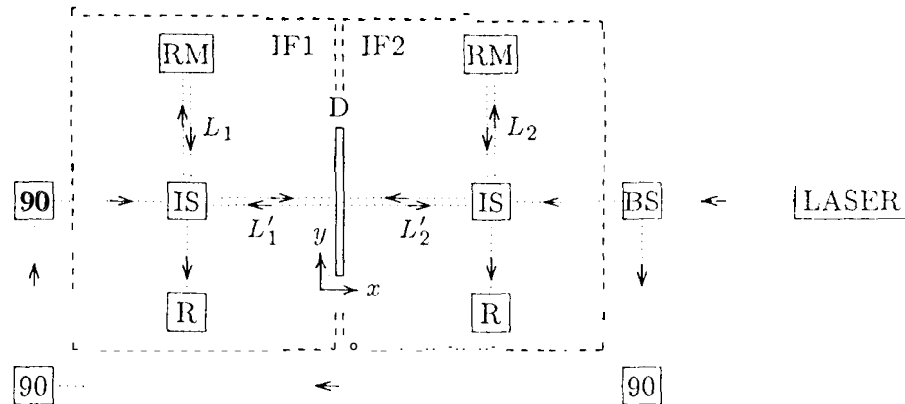


Figure 1. Schematic illustration of the dual interferometer system. System components are labeled as follows: D, silicon detector; RM, reference mirror; IS, interference splitter; BS, beam splitter; 90, 90° bend; R, receiver.

3. Interferometer Operation and Data Processing

Since the two surfaces of a detector are used as optical elements in the interferometer, they must have a mirror finish. The SIS detectors, which have aluminum contacts $\sim 2000\text{\AA}$ thick evaporated on polished silicon surfaces, have the necessary optical quality. A lens is used to focus the laser beam incident on the detector surface down to a diameter $< 0.5\text{ mm}$. With this small beam spot we can obtain an interference signal even when the detector surface is not exactly perpendicular to the beam (as can occur, for example,

if the detector surface is not flat). However, when the beam scans across a small piece of dust or other imperfection on the detector surface, the receiver can lose lock on the interference signal, introducing an unknown offset in the sequence of measurements. We have developed a procedure for identifying and correcting these discontinuities.

Our mapping procedure begins with a raster scan of the entire detector using horizontal scan lines and] making measurements along each line twice, first going left-to-right and then going back right-to-left. A χ^2 is calculated from the differences of the measurements along the two scans of the same line, and data from lines along which the χ^2 value exceeds a selected value are identified as containing discontinuities and are discarded.

We then rescan the entire detector using the same type of pattern but with vertical scan lines. After eliminating bad vertical lines and averaging, we have two detector maps (one horizontal, one vertical) in which each line that has been retained has no discontinuities, but which may have discontinuities between the different lines. The scan lines in the vertical map are then used to normalize (in the least squares sense) the scan lines in the horizontal map to eliminate the discontinuities. Similarly the horizontal map is used to normalize the vertical map. The two resulting maps are then averaged to obtain a final map which is free of discontinuities and complete except for a few discrete points corresponding to the intersections of bad rows in the horizontal map with bad columns in the vertical map. Point-by-point comparisons of the two, nearly-independent, normalized maps indicates that the rms errors in the measurements are $\lesssim 0.013 \mu\text{m}$.

The averaging of measurements obtained by scanning each line (horizontal and vertical) twice in opposite directions results in a first-order cancellation of any drifts (e.g., due to temperature variation) in the interferometer which may have occurred over the time required to produce the map.

Figure 2a contains an example of a thickness variation map obtained for a SIS detector (designated ACE004, 500 μm nominal thickness). The measurements were made on a 1 mm x 1 mm grid (approximately 6500 points, each measured 4 times). Such a mapping run takes approximately 6 hours and] is normally carried out overnight in order to minimize vibration noise due to other activities going on near the interferometer laboratory.

4. Comparison with an Accelerator Map

Detector ACE004 was scanned with a beam of ^{36}Ar ions with an energy $\sim 100 \text{ MeV/nucleon}$ at the National Superconducting Cyclotron Laboratory at Michigan State University in November 1994. We measured the energy loss, ΔE , and the residual energy, E' of each particle that penetrated ACE004. The ΔE measurements were averaged on a 3 mm x 3 mm grid to obtain a map of energy loss as a function of position. This map was converted to the thickness map shown in Figure 2b by dividing by the dE/dx value corresponding to the mean of E' measurements. Comparison of the accelerator map with the

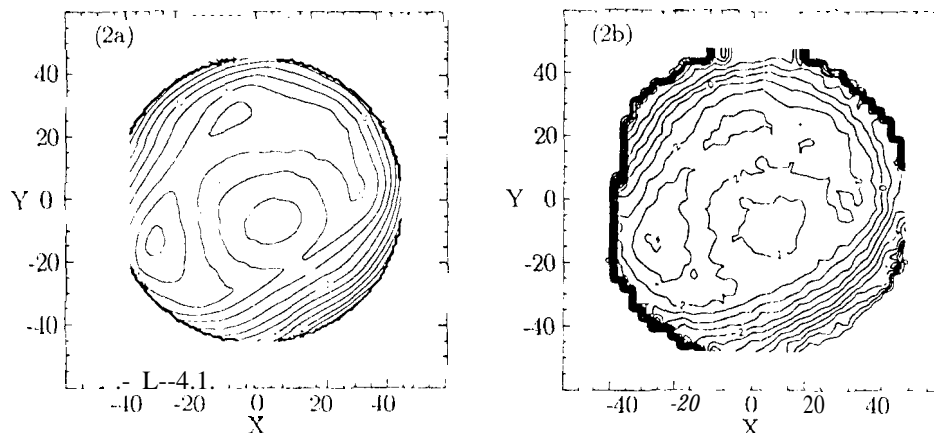


Figure 2. Maps of detector thickness variations made with the interferometer system (2a) and with accelerator beams of energetic ^{36}Ar nuclei (2b). Each map has a contour interval of $1\mu\text{m}$ and shows thickness differences from an arbitrary reference point. The X and Y scales are in mm.

interferometer map shows good agreement on both the qualitative features of the topography and on the quantitative details of the maps. The more jagged shape of the contours in the accelerator map is attributed to limited statistics and to the use of a coarser grid.

The interferometer measures the physical thickness of the detector, while the accelerator map based on measurements of ΔE is sensitive only to the active thickness. These two thicknesses can differ because of thin dead layers due to the ion implantation and metalization of the detector. The dead layer on each surface is expected to be $\sim 1\mu\text{m}$ thick and reasonably uniform. We are working on using the E' measurements from the accelerator run to obtain a direct measurement of the physical thickness of the ΔE detector. In addition, we are planning to carry out detector scans using collimated alpha particle sources to map the dead layers. Finally, we are testing modifications of the interferometer for making a single-point absolute thickness measurement using white-light interference.

We are grateful to R Radocinski and B. Sears for help with the data processing. The research described in this paper was supported by the National Aeronautics and Space Administration at the California Institute of Technology (under contract NA S5-32626 and grant NAGW-1919) and the Jet Propulsion Laboratory. Equipment funding was provided, in part, by the JPL Equipment and Instrumentation Committee.

References

- [1] Stone, E.C. *et al.*, in *Particle Astrophysics*, American Inst. of Phys. (New York) 1990.
- [2] Hewlett-Packard Corp., *Laser and Optics Users Manual*, 1992.